

Supporting Information for

Impact of *p*-type doping on charge transport in blade-coated small-molecule/polymer blend transistors

Aniruddha Basu^{a*}, Muhammad Rizwan Niazi^a, Alberto D. Scaccabarozzi^a, Hendrik Faber^a, Zuping Fei^b, Dalaver H Anjum^c, Alexandra F. Paterson^a, Olga Boltalina^d, Martin Heeney^e, Thomas D. Anthopoulos^{a*}

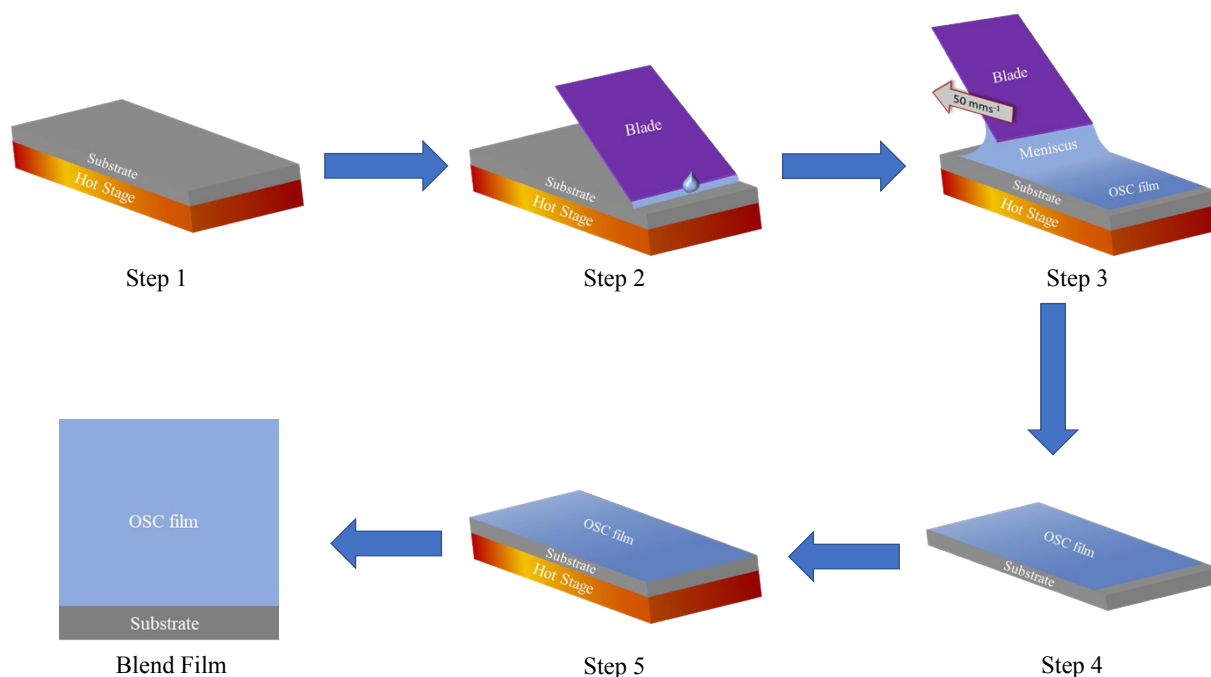


Figure S1. Schematic depiction of the blade-coating process. *Step 1* – Heating the substrate to 70 °C; *Step 2* – application of the blend solution on the substrate; *Step 3* – Blade-coating at 50 mm s⁻¹ speed while the substrate temperature is maintained at 70 °C; *Step 4* – Cooling the coated film by quenching the substrate to room temperature; *Step 5* – Annealing the solid film at 120 °C for 1 min then quenching back to room temperature.

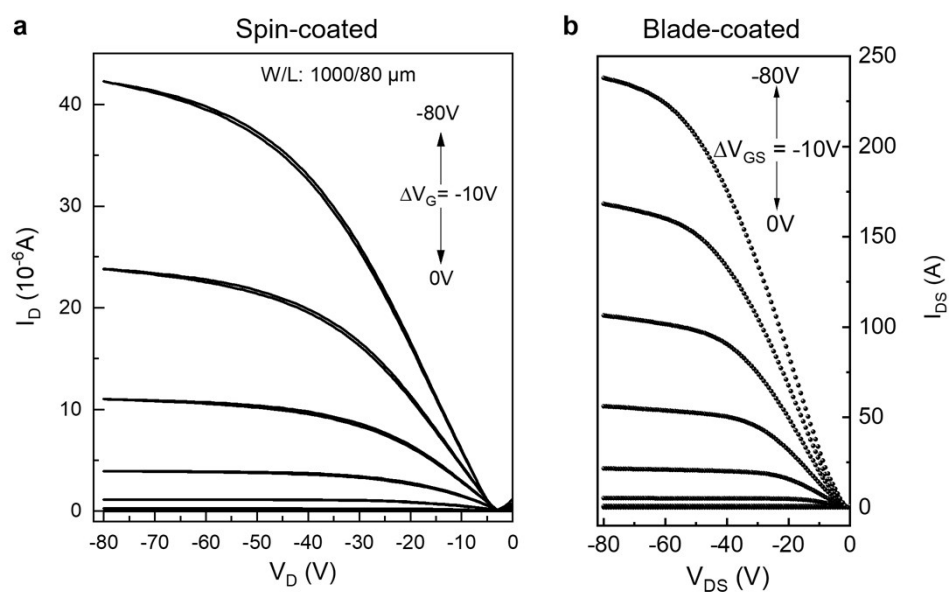


Figure S2. Output characteristics of spin-coated and blade-coated blend OTFTs.

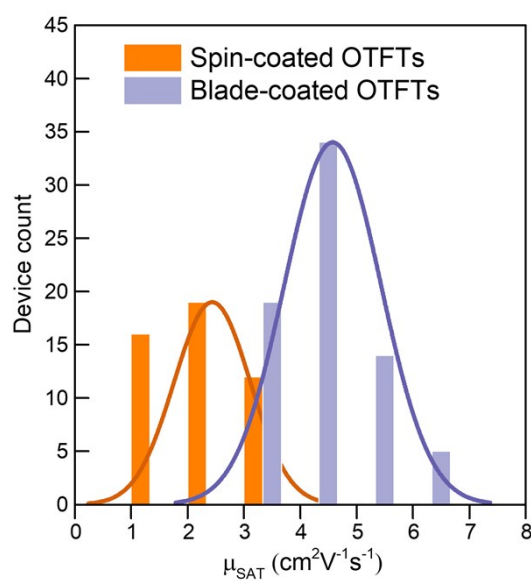


Figure S3. Histogram of calculated μ_{SAT} for the spin-coated and blade-coated blend OTFTs.

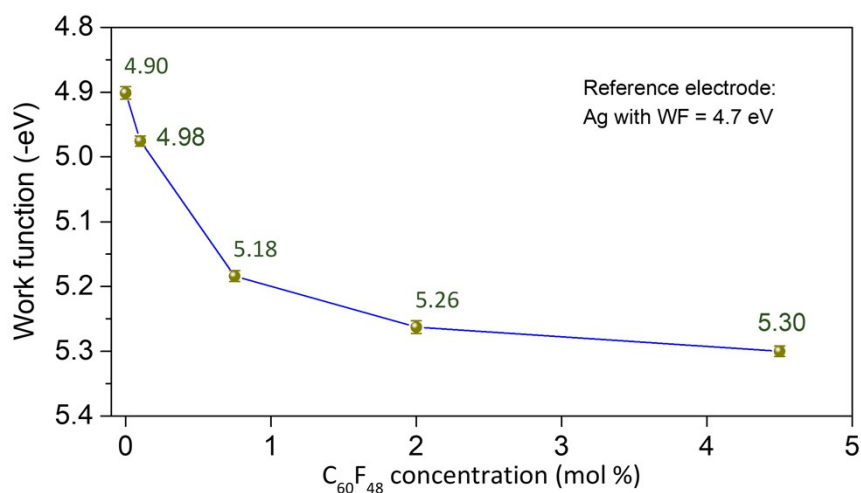


Figure S4. Workfunction (WF) measured via Kelvin Probe for the pristine and $C_{60}F_{48}$ -doped C_8 -BTBT: C_{16} IDT-BT blend films at different dopant concentrations.

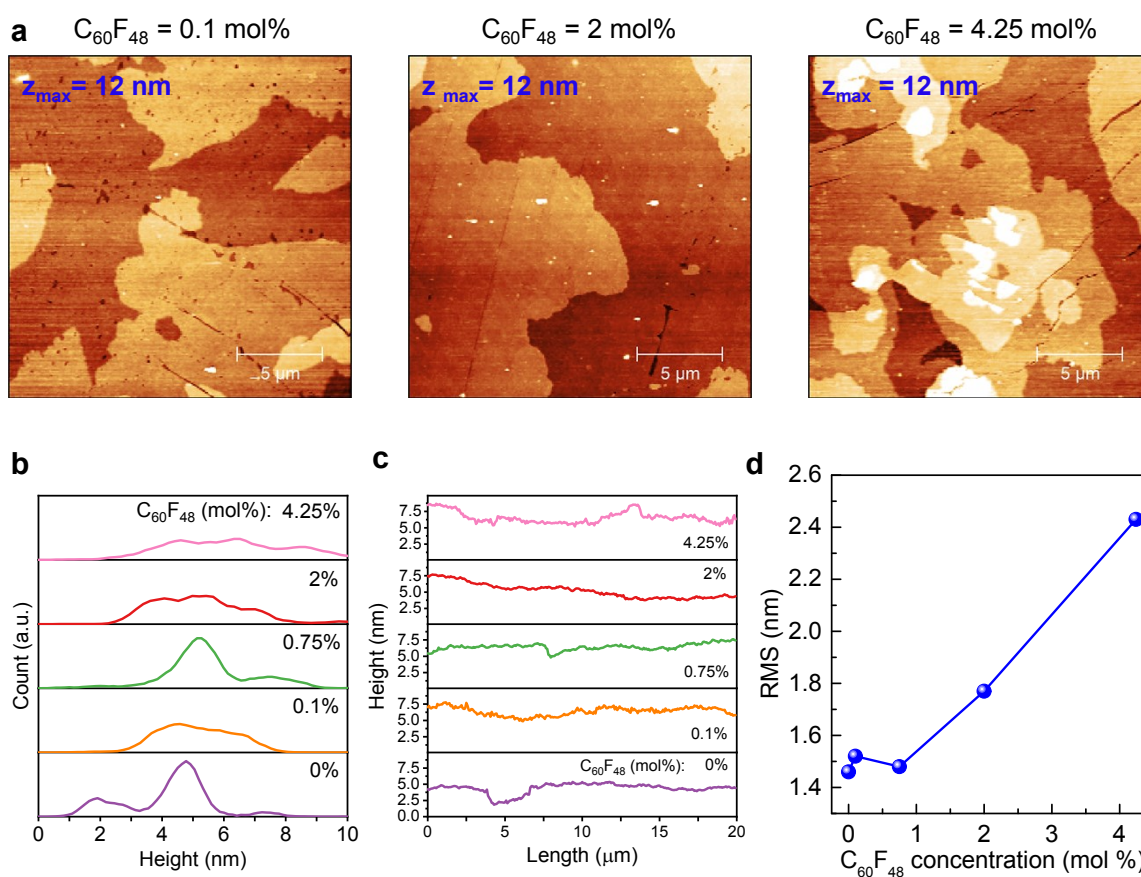


Figure S5. (a) AFM topography images of C_8 -BTBT: C_{16} IDT-BT blend layers with 0.1, 2 and 4.25 mol% $C_{60}F_{48}$. (b) Surface height distribution profiles extracted from the AFM topography images for all $C_{60}F_{48}$ concentrations studied. (c) Mean height distribution profile with respect to the scan area of the AFM topography images for the various $C_{60}F_{48}$ concentrations. (d) RMS of surface roughness of blend films as a function of $C_{60}F_{48}$ concentrations.

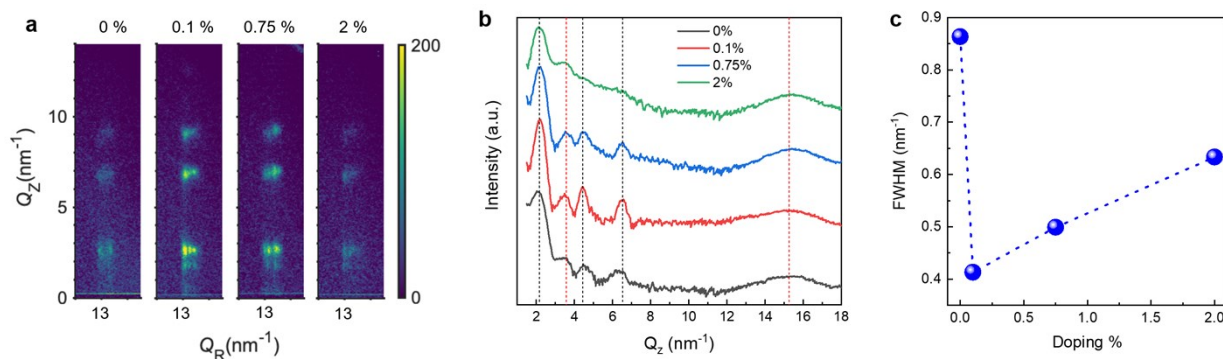


Figure S6. (a) Zoomed 2D GIWAXS patterns, and (b) Integrated intensity vs q (nm^{-1}) plots for out-of-plane Bragg sheets for blend films with different doping concentrations. (c) Plot of the FWHM of the (001) peak in (b) vs. $C_{60}F_{48}$ concentration.

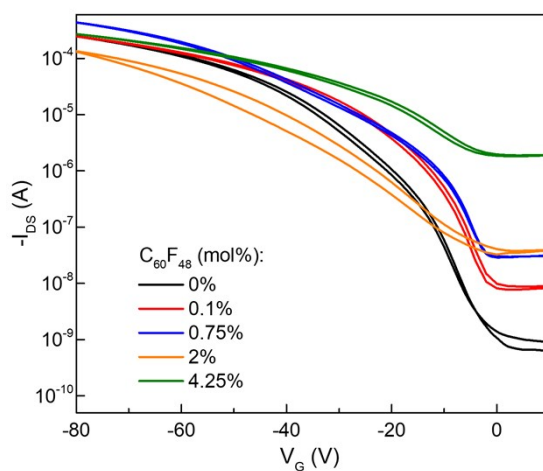


Figure S7. Transfer characteristics of the devices with different dopant concentrations.

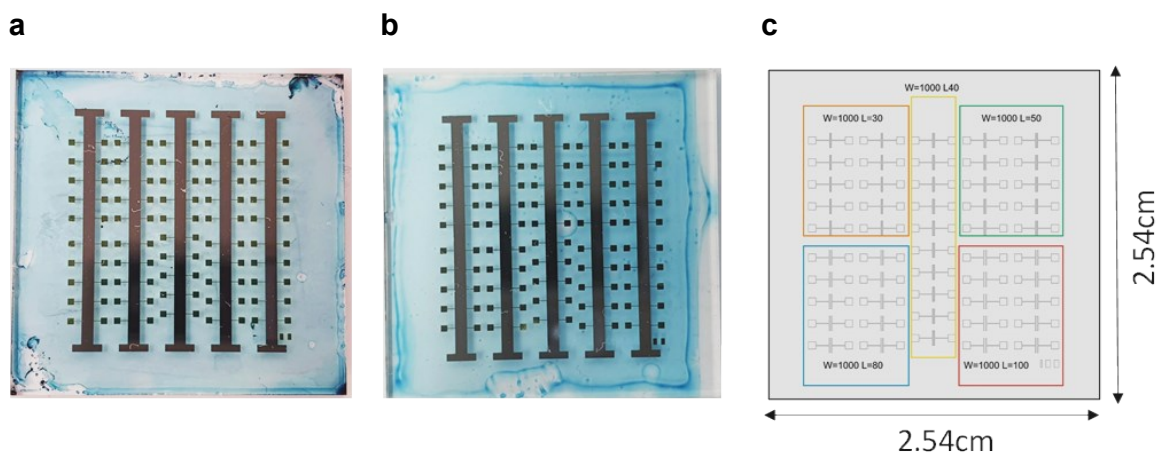


Figure S8. Photographs showing arrays of the spin-coated (a) and a blade-coated (b) C_8 -BTBT: C_{16} IDT-BT: $C_{60}F_{48}$ based OTFTs. (c) Schematic layout of the source-drain electrodes distributed across the substrate. The channel length (L) and width (W) dimensions in (c) are in μm .

Table S1. Typical values of ON channel current (I_{on}), ON/OFF channel current ratio ($I_{on/off}$), and threshold voltage (V_{TH}), measured for the different types of C_8 -BTBT: C_{16} IDT-BT based OTFTs studied here.

Device type	I_{on} (μA)	$I_{on/off}$	V_{TH} (V)
Spin-coated	43.29	4.1×10^5	37.89
Blade-coated (pristine)	247.73	4.7×10^5	23.24
Blade-coated (<i>p</i> -doped with 0.75 mol% $C_{60}F_{48}$)	422.31	1.47×10^4	24.39